Reproductive Biology and Endocrinology

RESEARCH

Open Access

Single-cell RNA sequencing reveals the effects of high-fat diet on oocyte and early embryo development in female mice

Qi Zhu[1,2†], Feng Li[3†], Hao Wang[3†], Xia Wang[1], Yu Xiang[1], Huimin Ding[1], Honghui Wu[1,5], Cen Xu[1], Linglin Weng[1,4], Jieyu Cai[1,4], Tianyue Xu[1,4], Na Liang[1,5], Xiaoqi Hong[1,2], Mingrui Xue[1,5] and Hongshan Ge[1,2,4,5*]

Abstract

Background Obesity is a global health issue with detrimental effects on various human organs, including the reproductive system. Observational human data and several lines of animal experimental data suggest that maternal obesity impairs ovarian function and early embryo development, but the precise pathogenesis remains unclear.

Methods We established a high-fat diet (HFD)-induced obese female mouse model to assess systemic metabolism, ovarian morphology, and oocyte function in mice. For the first time, this study employed single-cell RNA sequencing to explore the altered transcriptomic landscape of preimplantation embryos at different stages in HFD-induced obese mice. Differential gene expression analysis, enrichment analysis and protein-protein interactions network analysis were performed.

Results HFD-induced obese female mice exhibited impaired glucolipid metabolism and insulin resistance. The ovaries of HFD mice had a reduced total follicle number, an increased proportion of atretic follicles, and irregular granulosa cell arrangement. Furthermore, the maturation rate of embryonic development by in vitro fertilization of oocytes was significantly decreased in HFD mice. Additionally, the transcriptional landscapes of preimplantation embryos at different stages in mice induced by different diets were significantly distinguished. The maternal-to-zygotic transition was also affected by the failure to remove maternal RNAs and to turn off zygotic genome expression.

Conclusions HFD-induced obesity impaired ovarian morphology and oocyte function in female mice and further led to alterations in the transcriptional landscape of preimplantation embryos at different stages of HFD mice.

Keywords High-fat diet, Embryo development, Single-cell RNA sequencing, Obesity

†Qi Zhu, Feng Li and Hao Wang contributed equally Co-first authors.

*Correspondence:
Hongshan Ge
hongshange@njmu.edu.cn
[1]Reproductive Medicine Centre, The Affiliated Taizhou People's Hospital of Nanjing Medical University, Taizhou, China
[2]Graduate School, Nanjing Medical University, Nanjing, China
[3]Northern Jiangsu People's Hospital Affiliated to Yangzhou University, Yangzhou, China
[4]Graduate School, Nanjing University Of Chinese Medicine, Nanjing, China
[5]Graduate School, Dalian Medical University, Dalian, China

Introduction

Obesity is one of the causes of female infertility, the incidence of which is increasing worldwide [1]. Reproductive dysfunction in obese women primarily manifest as infertility and menstrual disorders, which may be associated with metabolic disorders such as polycystic ovary syndrome (PCOS), hyperlipidemia, insulin resistance, and hyperandrogenemia [2].

Female obesity is evidently associated with multiple adverse pregnancy outcomes and may lead to impaired fertility. It has been reported that obesity increases the risk of implantation failure and recurrent pregnancy loss [3]. In addition, an increase in atretic follicles and depletion of primordial follicles were observed in obese female rats [4]. One study showed that obese women undergoing in vitro fertilization had a 45% lower fertilization rate than normal weight women [5]. A meta-analysis by Sermondade et al. suggested that there is a reduced probability of live births in obese women following in vitro fertilization [6]. In contrast, a meta-analysis by Jungheim et al. showed that there was no difference in the chances of pregnancy after in vitro fertilization between obese donor oocyte recipients and those in the normal BMI range, suggesting that oocyte abnormalities may play a more dominant role in adverse pregnancies in obese women [7]. Therefore, investigating the underlying pathological mechanisms impairing oocyte and embryo developmental in obese women is crucial.

Early embryonic status serves as a critical index for predicting embryonic developmental potential and affecting embryonic implantation outcomes [8]. The oocyte, a large germ cell, plays a pivotal role in early embryonic development and is directly affected by surrounding granulosa cells, which provide the oocyte with essential hormones and nutrients to maintain its normal activity [9]. While previous studies have focused on the effects of obesity on embryonic reprogramming during pregnancy [10], its impact on the transcriptional landscape of preimplantation embryos remain poorly understood.

Mouse embryonic development closely mirrors that of humans, making it a favorable model to investigate preimplantation embryonic development in human beings [11–15]. In this study, we investigated the effects of obesity on follicular and early embryonic development using a high-fat diet (HFD)-induced obese murine model. Additionally, we employed single-cell RNA sequencing (scRNA-seq) to explore, for the first time, the altered transcriptomic landscape of preimplantation embryos at different developmental stages in HFD-induced obese mice. Our study primarily focuses on the effect of maternal obesity but normal paternal weight on preimplantation embryo development. Overall, these findings advance understanding of the impact of HFD-induced maternal obesity on ovarian and preimplantation embryonic development, laying the foundation for a more in-depth evaluation of its pathological mechanisms.

Materials and methods

Animals, diet, and experimental design

All procedures in this study were approved by the Ethical Committee and were conducted in accordance with relevant guidelines and regulations. Mice were maintained in specific pathogen-free conditions for 16 weeks, maintaining a 12-hour light/dark cycle, constant temperature, and controlled humidity. Three-week-old female C57BL/6 mice were randomly assigned to two groups: a normal diet (ND) group ($n=16$) and an HFD group ($n=24$). ND feed (10% fat Kcal %) and HFD (60% fat Kcal %) feed were purchased from Jiangsu Medicience Biomedical Co. All mice were housed individually, and feed was available ad libitum.

Collection of mouse oocytes and preimplantation embryos

Preimplantation embryos were collected from 19-week-old C57BL/6 female mice after mating with normal-diet male mice. To induce ovulation, female mice were intraperitoneally injected with 10 IU of pregnant mare serum gonadotropin (PMSG) (Ningbo Sansheng Pharmaceutical Corporation, Zhejiang, China), followed by 10 IU of human chorionic gonadotropin (hCG) (Ningbo Sansheng Pharmaceutical Corporation, Zhejiang, China) 48 h after PMSG priming. MII oocytes and embryos at each stage of preimplantation development were collected at defined time points after hCG administration: 14 h (MII oocyte), 46–48 h (late 2-cell), 68–70 h (8-cell), 88–90 h (early blastocyst), and 108–116 h (late blastocyst).

In vitro fertilization (IVF) of oocytes

For oocytes obtained as described in Section Collection of mouse oocytes and preimplantation embryos, cumulus cells were removed by digestion with hyaluronidase. Sperm obtained from the epididymis of normal-diet male mice were capacitated in HTF medium. The capacitated sperm were then added to the HTF medium containing cumulus-oocyte complexes for 4–6 h. Subsequently, sperm and embryos were cultured in fresh KSOM medium (Millipore) at 37 °C in a 5% CO_2 atmosphere. Two-cell, four-cell, eight-cell, morula, and blastocyst stage embryos were collected after 22–26, 48–50, 60–65, 70–75, and 96–100 h of culture, respectively.

scRNA-seq

scRNA-seq with Smart-seq2 was conducted on 16 preimplantation embryos samples fertilized in vivo (comprising five two-cell, five eight-cell, and six blastocysts) obtained as detailed in Section Collection of mouse oocytes and preimplantation embryos at different developmental stages by Tiangen Biochemical Technology

(Beijing) Co. Full-length cDNA and sequencing libraries were prepared following the Smart-Seq2 method. Briefly, single cells were lysed in a buffer containing free dNTPs and oligo (dT)-tailed oligonucleotides with a universal 5′ anchor sequence. Reverse transcription was performed by adding a few untemplated C-nucleotides to the 3′ end of the cDNA. A template switching oligo carrying two riboguanosines and an LNA-modified guanosine as the last base at the 3′ end hybridized to the untemplated C-nucleotide end. cDNA was amplified using KAPA HiFi DNA Polymerase in a limited number of cycles after first-strand synthesis. Sequencing libraries were then rapidly and efficiently constructed from the amplified cDNA using Tn5.

Serum triglycerides (TG) and total cholesterol (TC) tests

Prior to the experiment, mice in the ND and HFD groups were fasted overnight. Blood was collected from the orbital venous sinus of the mice the following morning (8:00–10:00 am) and placed into 1.5-mL EP tubes. The blood samples were allowed to stand at room temperature (RT) for 30 min, followed by centrifugation at 1800 g for 10 min and then at 1300 g for 2 min to collect the supernatant. Serum TG and TC levels were analyzed using the AU480 fully automated biochemical analyzer (Beckman Coulter, USA). Any remaining serum was stored at −80 °C to avoid repeated freeze-thaw cycles.

Serum insulin assay

Serum was separated after blood collection using the same method described above, following the manufacturer's instructions (ALPCO, USA). Readings were taken at an absorbance of 450 nm using a microplate reader, and values were calculated based on the standard curve.

Mouse glucose tolerance test (GTT)

Before the experiment, mice in the ND and HFD groups were fasted overnight. A 50% glucose injection solution was diluted to a 20% concentration with sterile saline and used for intraperitoneal injection at a volume of V = body weight (g)/100 (mL) for each mouse. Blood samples were taken from the tail vein at 0, 15, 60, and 120 min post-injection, discarding the first drop and measuring the second drop using a blood glucose (BG) analyzer. A GTT curve was plotted, and the area under the curve (AUC) was calculated using the following formula: $AUC = (BG_{0min}+BG_{30min}) \times 30/2 + (BG_{30min}+BG_{60min}) \times 30/2+(BG_{60min}+BG_{90min}) \times 30/2+(BG_{90min}+BG_{120min}) \times 30/2$.

Follicle count

Ovarian was collected, fixed in 4% paraformaldehyde for 24 h, then embedded in paraffin, followed by serially sectioned at a thickness of 5 μm. Ovarian tissue was stained with H&E and counted every five sections (a total of 8–12 sections per ovary). The histological morphology of the ovaries was observed under the microscope. Follicles include primordial follicles, primary follicles, secondary follicles, antral follicles and atretic follicles. Atretic follicles were characterized by consolidation of granulosa cells, disintegration of cumulus cells, abnormal division of oocytes and thickening and vitrification of the zona pellucida.

Transmission electron microscopy (TEM)

Ovary samples were obtained within 3 min after the mice were sacrificed, after which the blood clots were removed and the samples were placed in an electron microscope fixative. After fixation at RT for 2 h, the samples were stored at 4 °C and subsequently imaged by transmission electron microscopy (HITACHI, Japan).

Statistical analysis

GraphPad Prism was employed for statistical analysis, and data were presented as mean ± standard deviation (SD). When the data were normally distributed, differences between the two groups were analyzed using Student's t-test. One-way analysis of variance and Student-Newman-Keuls multiple comparison tests were applied to analyze differences among three or more groups. P-value < 0.05 was considered statistically significant.

Results

Effects of HFD-induced obesity on systemic metabolism, ovarian morphology, and IVF embryo development

Upon exposure to a HFD for 16 weeks, adult female mice exhibited a pronounced increase in body weight, as evidenced by the obese phenotype (Fig. 1A) and the weight gain curve (Fig. 1B). Serum biochemical analysis of 19-week-old mice following an 8-hour fast revealed significant increases in TG (Fig. 1C), TC (Fig. 1D), and insulin (Fig. 1E) levels. Glucose tolerance was assessed after an 8-hour fast, with results indicating a significantly higher area under the glucose tolerance curve in the HFD group than in the ND group (Fig. 1F and G). These results suggested impaired glucolipid metabolism and insulin resistance in female HFD mice. HE staining was used to observe ovarian morphology (Supplementary Fig. 1A). The results showed that the number of follicles in the ovaries of HFD mice was decreased and the proportion of atretic follicles was obviously increased compared with the ND mice (Supplementary Fig. 1B and C). Transmission electron microscopy further elucidated morphological differences between ovarian follicles of the two dietary groups. Follicles in the ND group exhibited an oval configuration with granulosa cells (GCs) that were uniformly arranged and densely packed, exhibiting

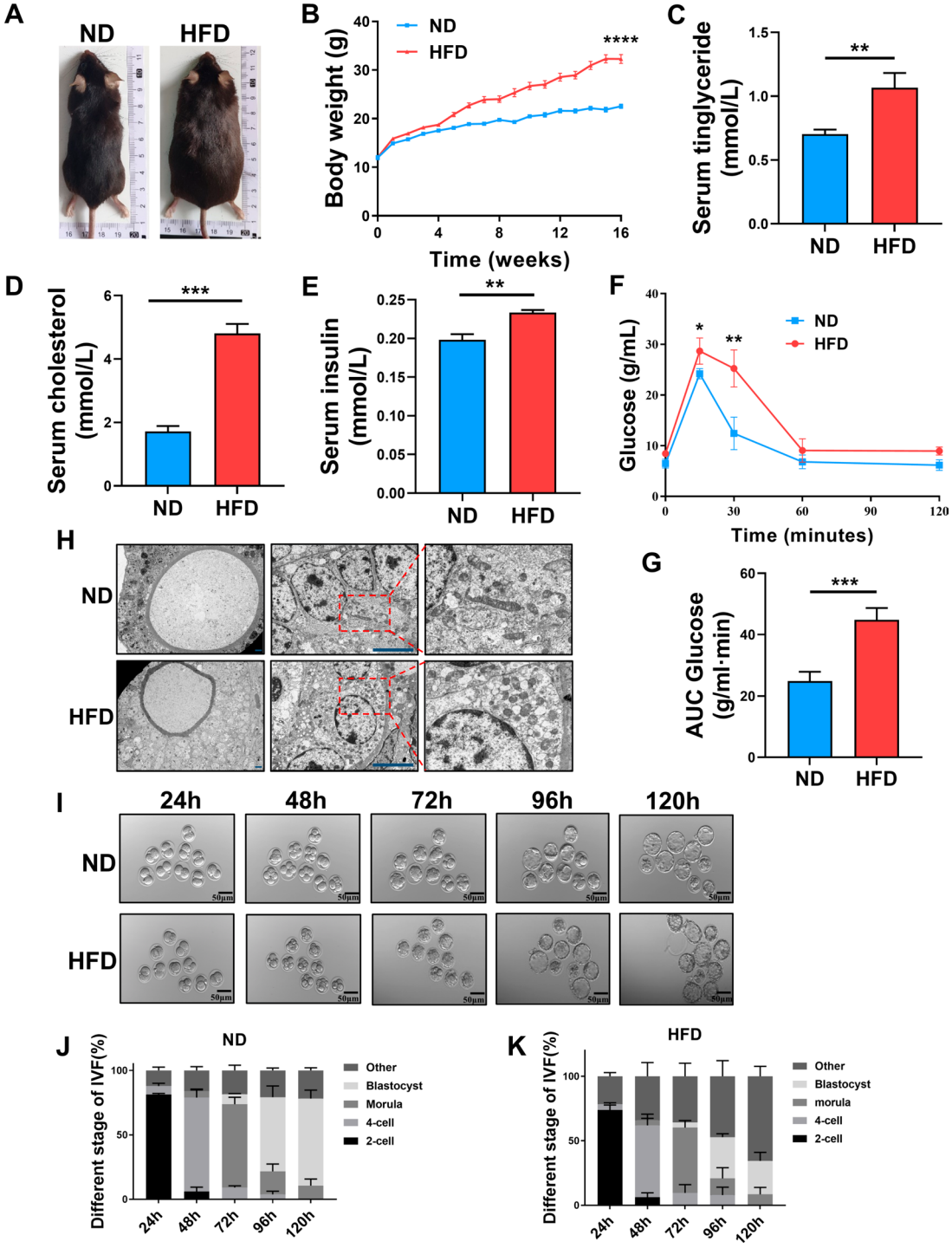

Fig. 1 Effects of HFD-induced obesity on metabolism, ovarian morphology, and IVF embryo development were explored. (**A**) Phenotypes of mice in each group. (**B**) Body weight growth curves of mice in each group treated with ND ($n=16$) or HFD ($n=24$) for 16 weeks. Levels of serum triglycerides (**C**), total cholesterol (**D**), and insulin (**E**) in different groups of mice after 8 h of fasting ($n=3$). Change in glucose tolerance curves (**F**) and area (**G**) under the curve in each group of mice after 8 h of fasting ($n=4$). (**H**) Representative transmission electron microscopy images of mice in the ND and HFD groups ($n=3$). Scale bar: 5 μm. Morphology (**I**) of early embryo development in vitro and proportion of embryos at different stages (**J** and **K**) of in vitro culture in ND and HFD mice ($n=3$). Scale bar: 50 μm. Error bars indicate mean ± SEM. $^{*}P<0.05$, $^{**}P<0.01$, $^{***}P<0.001$, $^{****}P<0.0001$

distinct cell boundaries (Fig. 1H). Conversely, follicles in the HFD group presented with irregular contours, with GCs arranged haphazardly, expanded intercellular spaces, and indistinct cell boundaries (Fig. 1H). Additionally, GCs in the HFD group exhibited vacuolated mitochondria. We further explored the effect of HFD on the developmental maturation rate of IVF embryos in mice. The results showed a markedly lower blastocyst rate in the HFD group (Fig. 1I-K). These comprehensive findings collectively highlight the detrimental impact of a HFD on the functional integrity of the mouse ovary and systemic metabolism, suggesting a causal relationship between HFD consumption and ovarian dysfunction.

Single-cell transcriptome analysis of preimplantation embryos from HFD-induced obese mice

To better understand the effects of HFD-induced obesity on preimplantation embryo development, we conducted genome-wide mRNA expression analysis of single embryos from the 2-cell stage to the blastocyst stage in the HFD and matched ND groups. A total of 16 preimplantation embryo samples ranging from the 2-cell stage to the blastocyst stage were harvested (Fig. 2A). Principal component analysis (PCA) results demonstrated better separation of transcription profiles of cells from different preimplantation stages (Fig. 2B). Differentially expressed genes (DEGs) were identified based on thresholds of P-value < 0.05 and absolute fold change > 2. The DEG heatmap revealed separate clustering of gene expression patterns after unsupervised clustering (Fig. 2C), suggesting significant differences in embryonic transcriptional landscapes at different preimplantation stages.

Effects of HFD-induced obesity on the transcriptional landscape of the 2-cell stage

Next, we analyzed the impact of HFD-induced obesity on the transcriptional landscapes of preimplantation embryos at different stages. Further analysis of PCA and heatmap of the 2-cell stage revealed notable gene expression differences between the ND and HFD groups (Fig. 3A and D). A total of 258 DEGs were identified in the HFD group, comprising 131 up- and 127 downregulated genes, based on thresholds of P-value < 0.05 and absolute fold change > 2 (Fig. 3B). These DEGs were depicted in the volcano plot (Fig. 3C). We performed a functional enrichment analysis of all DEGs using Gene Ontology biological process (GO-BP), Gene Ontology cellular component (GO-CC), and Gene Ontology molecular function (GO-MF). GO-BP analysis revealed that upregulated DEGs were significantly enriched in apoptosis, glycolytic, and cell cycle processes (Fig. 3E), whereas downregulated genes were associated with cytoplasmic translation, ribosome biogenesis, and mitochondrial gene expression (Fig. 3G). Regarding GO-CC, upregulated genes in the HFD group were primarily found in exocytic vesicles and the perinuclear region of the cytoplasm (Fig. 3E), whereas downregulated genes were predominantly localized in ribosomes and RNA polymerase complexes (Fig. 3G). GO-MF analysis showed that these upregulated genes were mainly involved in ion channel regulator activity and RNA methyltransferase activity (Fig. 3E), whereas key downregulated genes were associated with structural constituents of ribosomes and transcription factor binding (Fig. 3G).

Kyoto Encyclopedia of Genes and Genomes (KEGG) pathway analysis indicated that upregulated genes in the

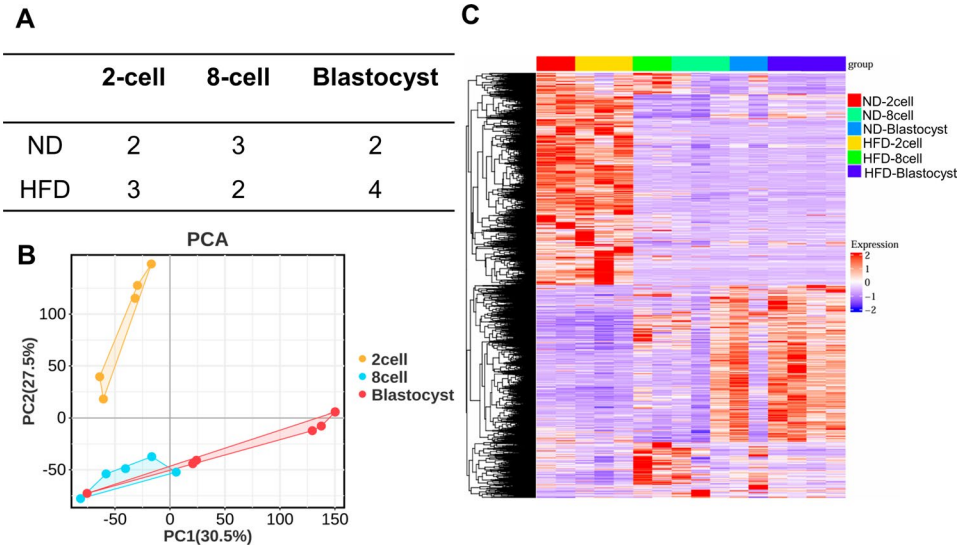

Fig. 2 Single-cell sequencing (scRNA-seq) was used to detect different stages of preimplantation embryos in HFD-induced obese mice. (**A**) Number of preimplantation embryo samples at different stages used for scRNA-seq. (**B**) Two-dimensional PCA representation. (**C**) Heatmap showing hierarchical clustering of highly viable genes

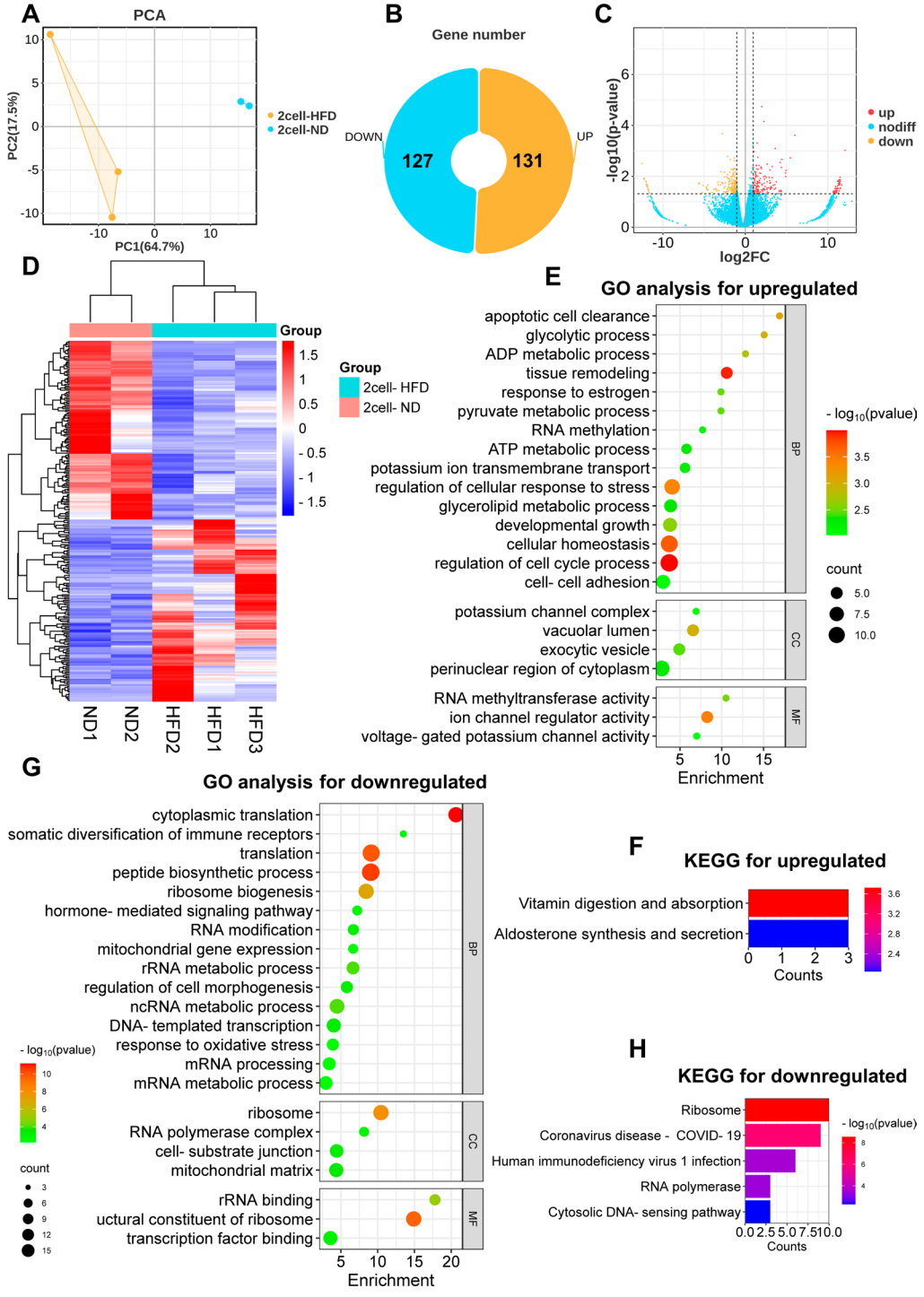

Fig. 3 DEGs of 2-cell stage preimplantation embryos were analyzed. PCA chart (**A**), pie plot (**B**), and volcano plot (**C**) showing 131 up- and 127 downregulated differentially expressed genes (DEGs) ($P < 0.05$ and absolute fold change > 2) in 2-cell stage preimplantation embryos from the ND ($n = 2$) and HFD groups ($n = 3$). (**D**) Heatmap showing hierarchical clustering of highly viable genes. GO analysis for the up- (**E**) and downregulated (**G**) DEGs in 2-cell stage preimplantation embryos. Major KEGG analysis for the up- (**F**) and downregulated (**H**) DEGs in 2-cell stage preimplantation embryos

HFD group were mainly involved in vitamin absorption and aldosterone secretion (Fig. 3F), whereas downregulated genes were enriched in ribosomal and RNA polymerase and cytosolic DNA-sensing pathways (Fig. 3H). These findings collectively suggest metabolic disorders and abnormal gene transcription in 2-cell embryos exposed to HFD.

Effects of HFD-induced obesity on the transcriptional landscape of the 8-cell stage

We next focused on the effects of HFD-induced obesity on the transcriptional landscapes of 8-cell stages. PCA and heatmap analysis revealed significant differences in gene expression between the ND and HFD groups (Fig. 4A and D). A total of 358 DEGs were identified in the HFD group, comprising 58 upregulated and 300 downregulated genes, based on thresholds of P-value < 0.05 and absolute fold change > 2 (Fig. 4B). These DEGs were visualized in the volcano plot (Fig. 4C). GO-BP analysis indicated that upregulated DEGs were enriched in regulating inflammatory responses and protein catabolic processes (Fig. 4F), whereas downregulated genes were associated with fatty acid metabolism, embryonic organ development, and cell proliferation (Fig. 4G). Regarding GO-CC analysis, upregulated genes in the HFD group were predominantly found in coated vesicle (Fig. 4F), whereas downregulated genes were localized to the cell division site, nuclear matrix, and mitochondrial outer membrane (Fig. 4G). GO-MF analysis suggested involvement of upregulated genes in molecular function inhibitor activity and nuclear receptor binding (Fig. 4F), whereas key downregulated genes were associated with DNA-binding transcription factor binding and cell adhesion (Fig. 4G).

KEGG pathway analysis revealed that upregulated genes were mainly involved in autophagy and mRNA surveillance pathways (Fig. 4E), whereas downregulated genes were enriched in fatty acid metabolism, glycolysis, and the PI3K-Akt signaling pathway (Fig. 4H). These findings indicate potential poor embryonic development and metabolic disorders in 8-cell embryos exposed to HFD.

Effects of HFD-induced obesity on the transcriptional landscape of the blastocyst stage

Our next focus was on the impact of HFD-induced obesity on the transcriptional landscapes of blastocyst stages. Significant differences in gene expression were observed between the ND and HFD groups, as evidenced by PCA and heatmap analysis of the blastocyst stage (Fig. 5A and D). A total of 588 DEGs were identified in the HFD group, comprising 32 up- and 556 downregulated genes, based on thresholds of P-value < 0.05 and absolute fold change > 2 (Fig. 5B). Visualization of these DEGs was provided through the volcano plot (Fig. 5C). GO-BP analysis indicated that upregulated DEGs were associated with the regulation of inflammatory responses, organic acid biosynthesis, and brain development (Fig. 5E), whereas downregulated genes were enriched in autophagy, glycolysis, cell proliferation, and non-coding RNA processing (Fig. 5G). Regarding GO-CC analysis, upregulated genes in the HFD group were mainly found in glutamatergic synapse (Fig. 5E), whereas downregulated genes were predominantly localized in autophagosomes and the mitochondrial outer membrane (Fig. 5G). GO-MF analysis suggested the involvement of upregulated genes in oxidoreductase activity and chromatin binding (Fig. 5E), whereas key downregulated genes were associated with structural constituents of transcription factor binding and miRNA binding (Fig. 5G).

KEGG pathway analysis revealed that upregulated genes were primarily involved in carbon metabolism, whereas downregulated genes were enriched in autophagy, ferroptosis, and thyroid hormone signaling pathways (Fig. 5F). These results indicated that blastocyst embryos in the HFD group may have disturbed cellular function.

Interference of HFD-induced obesity for maternal-to-zygotic transition in embryos

Zygote genome activation (ZGA), the initiation of gene expression following fertilization, is a crucial process in preimplantation embryo development [16]. The ZGA wave in mice occurs predominantly after the 2-cell stage and before the 8-cell stage. Therefore, we analyzed DEGs at the 8-cell versus the 2-cell stage in the HFD and ND groups, respectively, which revealed differences in ZGA. Among 1126 DEGs, 460 (40.9%) were not activated in the HFD group (Fig. 6A), whereas 1065 DEGs were abnormally upregulated, suggesting that the ZGA process may be disturbed after HFD-induced obesity (Fig. 6A). Functional enrichment analysis of the 460 DEGs not activated in the HFD group using GO analysis revealed associations with cell-cell adhesion, cell activation, and glutathione metabolic processes (Fig. 6B). KEGG analysis indicated that the DEGs were mainly enriched in adherens junctions, oxidative phosphorylation, and glutathione metabolism (Fig. 6C). Based on the information in the Search Tool for the Retrieval of Interacting Genes (STRING) database and Molecular Complex Detection (MCODE) plug-in in Cytoscape software, the most significant cluster 1, containing 17 DEGs, was identified in the protein-protein interaction (PPI) network formed by 460 DEGs (not activated in the HFD group) (Fig. 6E). The GO enrichment analysis showed that these genes were mainly associated with cell activation, homotypic cell-cell adhesion, and response to extracellular stimuli (Fig. 6F), showing highly relative response at the 2-cell stage after HFD-induced obesity. In addition, we performed

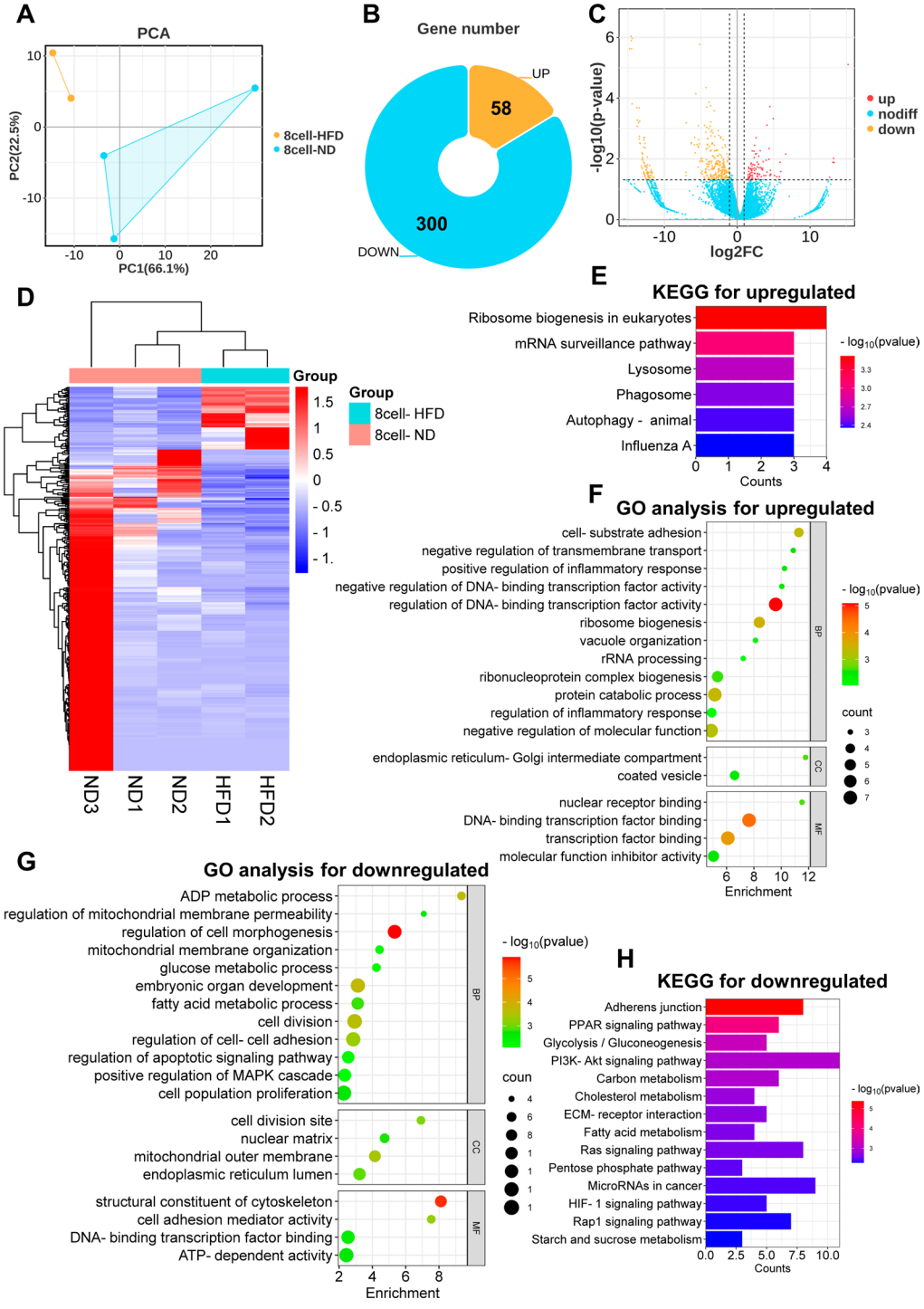

Fig. 4 DEGs of 8-cell stage preimplantation embryos were analyzed. PCA chart (**A**), pie plot (**B**), and volcano plot (**C**) showing 58 up- and 300 down-regulated DEGs ($P < 0.05$ and absolute fold change > 2) in 8-cell stage preimplantation embryos from the ND ($n = 3$) and HFD groups ($n = 2$). (**D**) Heatmap showing hierarchical clustering of highly viable genes. GO analysis for the up- (**F**) and downregulated (**G**) DEGs in 8-cell stage preimplantation embryos. Major KEGG analysis for the up- (**E**) and downregulated (H) DEGs in 8-cell stage preimplantation embryos

enrichment analyses of 1065 DEGs abnormally activated after HFD. The results showed that these upregulated genes were mainly associated with DNA damage and repair, autophagy, cellular stress and ferroptosis, which further proved the injury response after HFD (Supplementary Fig. 2A and B).

Another crucial event during the maternal-to-zygotic transition (MZT) is the clearance of maternal mRNAs

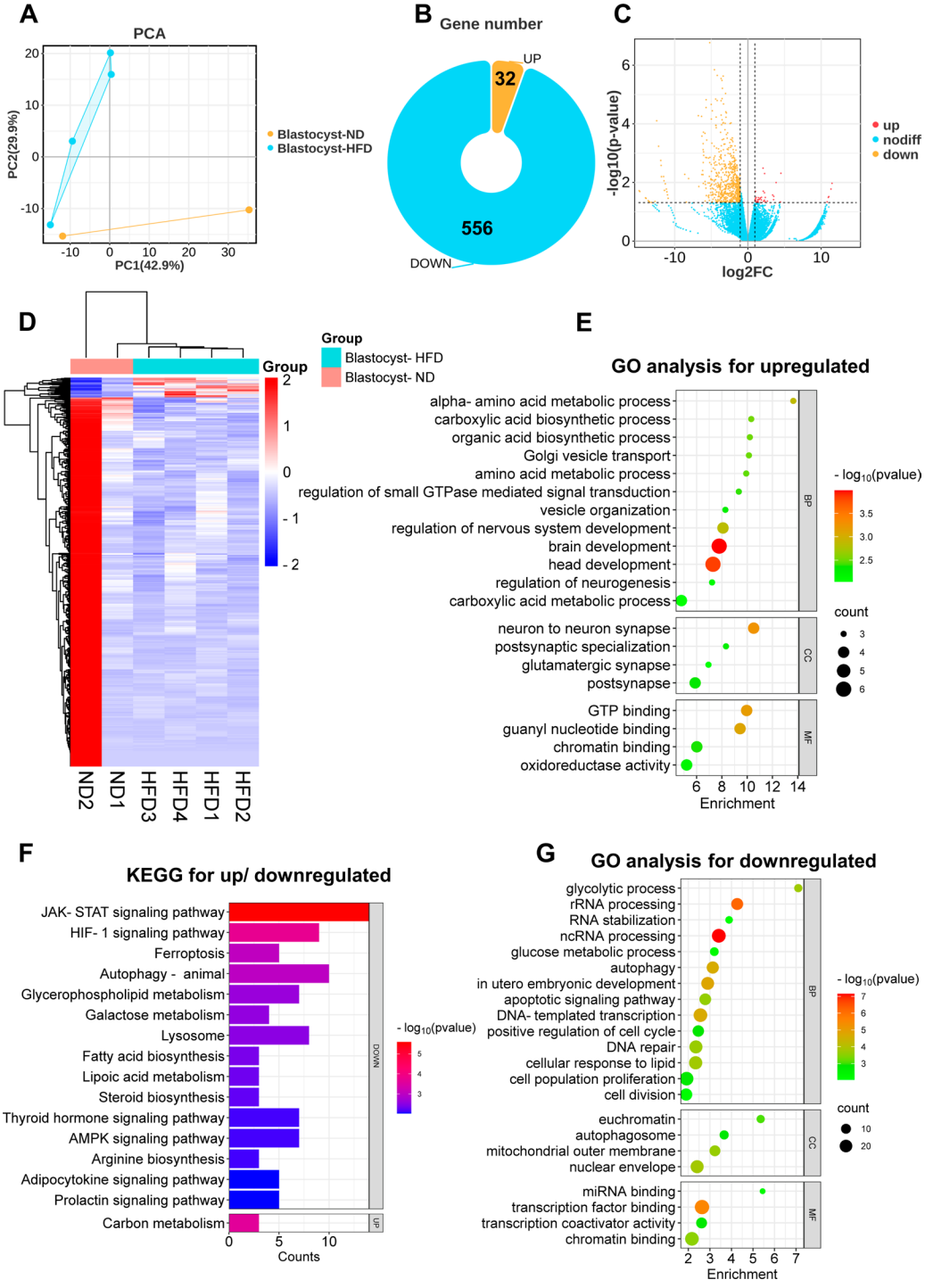

Fig. 5 DEGs of blastocyst stage preimplantation embryos were analyzed. PCA chart (**A**), pie plot (**B**), and volcano plot (**C**) showing 32 up- and 556 downregulated DEGs ($P < 0.05$ and absolute fold change > 2) in blastocyst stage preimplantation embryos from the ND ($n = 2$) and HFD groups ($n = 4$). (**D**) Heatmap showing hierarchical clustering of highly viable genes. GO analysis for the up- (**F**) and downregulated (**G**) DEGs in blastocyst stage preimplantation embryos. Major KEGG analysis for the up- (**E**) and downregulated (**H**) DEGs in blastocyst stage preimplantation embryos

[17]. Compared with the ND group, HFD-induced obesity resulted in embryos failing to downregulate 24.1% (476/1973) of maternal RNAs at the 8-cell stage and having 1026 DEGs abnormally downregulated (Fig. 6D), potentially impairing preimplantation embryo development. Enrichment analysis revealed that the 476 DEGs that failed to be downregulated in HFD mice were mainly associated with DNA damage, RNA modification,

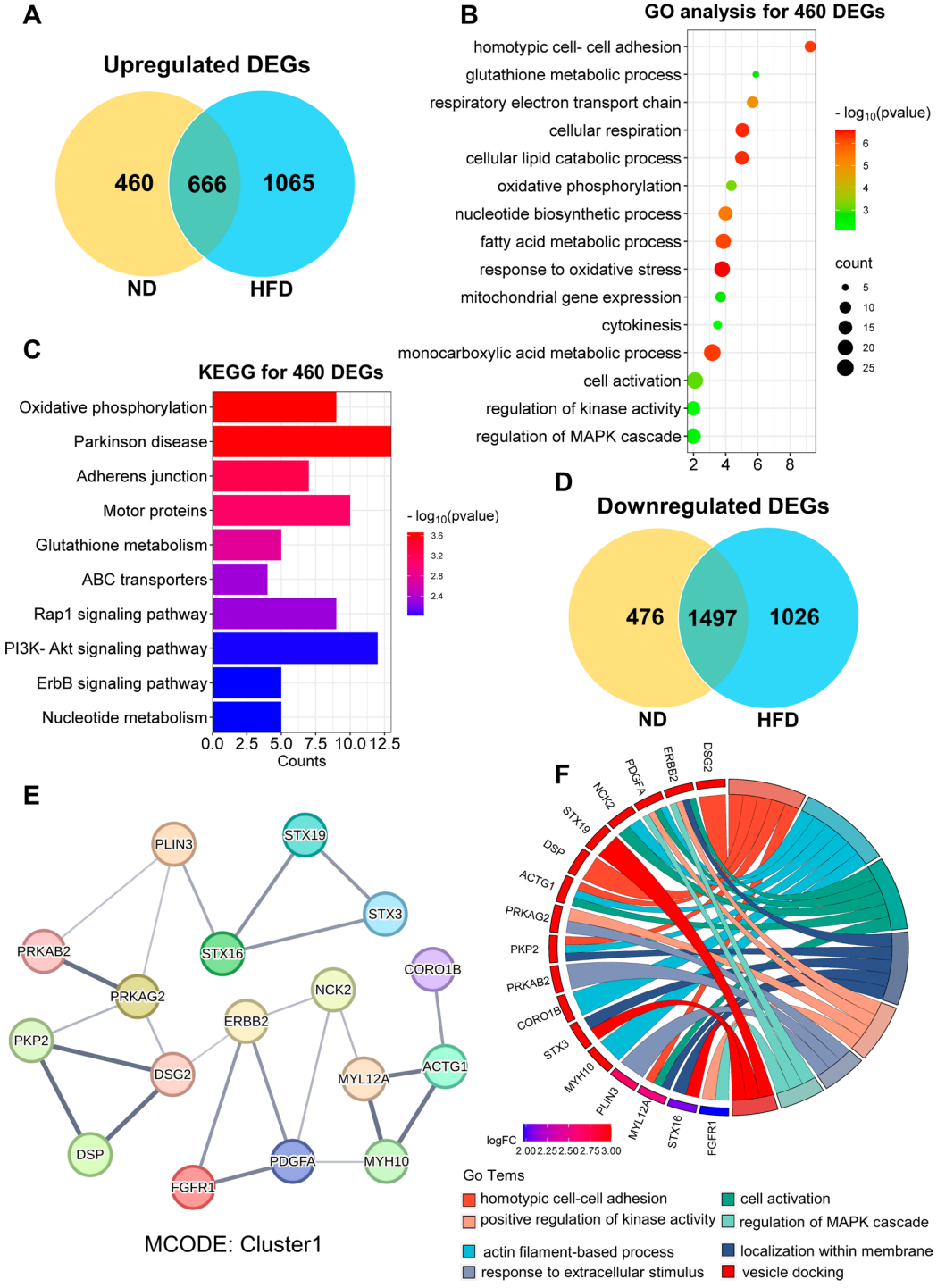

Fig. 6 Maternal-to-zygotic transition was altered in preimplantation embryos of HFD and ND mice. (**A**) Venn diagram of upregulated zygote genome activation (ZGA) DEGs at the 8-cell stage compared with the 2-cell stage in both ND and HFD mice. (**B**) GO analysis for 460 ZGA DEGs not upregulated in HFD mice. (**C**) Major KEGG analysis for 460 ZGA DEGs not upregulated in HFD mice. (**D**) Venn diagram of downregulated DEGs at the 8-cell stage compared with the 2-cell stage in both ND and HFD mice. (**E**) The top cluster 1 was derived from the protein-protein interactions network (PPIs) with the Molecular Complex Detection (MCODE) algorithm. (**F**) GO analysis for 17 DEGs in top cluster 1

reactive oxygen species metabolism, and adipocytokine signaling pathways (Supplementary Fig. 2C and D). In contrast, the 1026 DEGs specifically downregulated in HFD mice were primarily involved in cell morphogenesis and establishment of polarity, embryonic development, cell mitosis and metabolic pathways (Supplementary Fig. 2E and F). These findings suggest that HFD-induced obesity might interfere with MTZ.

Discussion

In this study, we established a female mouse model of obesity induced by 16 weeks of HFD. Our findings demonstrated glycolipid metabolism disorder, follicular structural abnormalities, and reduced embryonic development maturation in the HFD group of mice. Moreover, through scRNA-seq of preimplantation embryos at different stages in the ND and HFD groups, we, for the first time, revealed disruptions in various biological processes such as glycolipid metabolism, cell cycle, apoptosis, autophagy, and ferroptosis, along with potential disturbances in MTZ. These results provide a preliminary basis for an in-depth investigation of the mechanisms underlying HFD-induced obesity's impact on ovarian oocyte and preimplantation embryo development.

Obesity is a global health issue with detrimental effects on various human organs, including the reproductive system [18]. With rising standards of living, humans are gradually inclined to an HFD, which is the main cause of increasing obesity rates. Several studies have shown that feeding mice with HFD can successfully induce obesity [19, 20]. In this study, we induced obesity in female mice by HFD for 16 weeks and observed excessive weight gain, disrupted glucolipid metabolism, and insulin resistance in HFD mice, consistent with a previous report [20]. Obese women have been reported to have significantly lower ovarian reserve [21, 22]. Our results showed that follicles in the HFD group presented with irregular contours, GCs arranged haphazardly with expanded intercellular spaces and containing vacuolated mitochondria, and indistinct cell boundaries, consistent with the report of Skaznik-Wikiel et al. in which HFD-induced obesity reduced the number of primordial follicles and increased the number of atretic follicles, suggesting that obesity resulted in a poor ovarian microenvironment [23]. The rate of embryonic development at different stages after IVF of oocytes is a crucial indicator for assessing oocyte quality. Previous studies have shown lower fertilization rates, poor blastocyst development, and high apoptotic index in the blastocysts of HFD-fed mice, suggesting impaired in vitro developmental potential of oocytes [24]. Luzzo et al. also found that the degradation rate of HFD-fed mouse embryos was higher during in vitro culture [25], consistent with our results demonstrating significantly lower developmental maturation rate of in vitro fertilized embryos in the HFD group, which suggested that HFD may adversely affect oocyte quality in mice.

After fertilization, finely regulated cleavage cellular events determine the completion of embryogenesis to produce living offspring. Any disruption of these events can lead to embryo developmental defects, and the origin of these developmental problems could be impaired oocyte quality [15, 26]. Recent studies have suggested that impaired embryonic developmental competence may result from three adverse effects primarily associated with oocytes: (1) mitochondrial dysfunction, (2) lipotoxicity, and (3) epigenetic dysregulation [15]. Clinical studies have reported that blastocysts from women with a high dietary intake of fat have altered metabolism and increased lipid content [27, 28]. Meanwhile, in the HFD mouse model, ROS levels were elevated in oocytes, indicating oxidative stress and consequent mitochondrial dysfunction [8]. Epigenetic dysregulation may be equally involved in the adverse effects of the maternal high-fat diet on embryonic development. Several previous studies have identified altered DNA methylation status of metabolism-related and development-related genes [29, 30]. These findings revealed complex mechanisms by which HFD impaired oocytes and preimplantation embryos. Notably, our enrichment analyses of DEGs from preimplantation embryos at different stages of HFD similarly scanned for alterations in these biological processes.

Recently, scRNA-seq has been widely applied to study preimplantation embryonic development [13, 31, 32]. Several recent studies using RNA sequencing to study HFD-induced maternal obesity mostly evaluated the effects of obesity on the transcriptional landscape of the murine ovary or placenta but not alterations in the preimplantation embryo [33, 34]. Previous studies have mostly focused on the effects of male obesity on embryonic RNA transcriptional profiles [35]. The results of the blastocyst study by Hedegger et al. suggested that the sex-specific programming effects of parental obesity began at the preimplantation stage and revealed an association between specific alterations in the sperm miRNA profile and the programming effects of paternal obesity [36]. We uniquely used scRNA-seq to explore dynamic changes in the transcriptional landscape of preimplantation embryos from the 2-cell to blastocyst stage in response to HFD-induced obesity in maternal mice (paternal weight normal). Cluster analysis of transcriptomes from preimplantation embryos at almost all stages showed that the transcriptome profiles of the embryos were primarily segregated according to the embryonic stage, followed by clustering into different dietary treatment conditions (ND or HFD), which suggested significant differences in the embryonic transcriptional landscapes at different preimplantation stages.

Parental obesity has a negative impact on embryo development [37, 38]. A previous study revealed markedly reduced number of embryos that developed on time to the blastocyst stage in all groups of obese parents compared with those of lean parents [39]. Obese mothers produce embryos with reduced developmental competence, consistent with previous findings on obesity in animals and humans [25, 40, 41]. Indeed, evidence from rodent studies suggests that maternal obesity leads to reduced blastocyst rates, downregulation of key metabolic genes, slower embryo development, and adverse effects on fetal health [41, 42]. In this study, we found significant differences in the transcriptional landscapes of preimplantation embryos at the same developmental stage in mice with different dietary treatments (ND or HFD). Our results indicated that DEGs in the 2-cell stage of the HDF group were mainly associated with apoptosis, glycolysis, and ribosome function, whereas those in the 8-cell stage were mainly enriched for negative regulation of cell proliferation, fatty acid metabolism, mitochondrial function, and autophagy. DEGs in the blastocyst stage of the HFD group were mostly associated with autophagy, glycolytic processes, cell proliferation, and mitochondria, indicating possible metabolic disorders and developmental delays in preimplantation embryos. Notably, our KEGG enrichment analysis showed that downregulated DEGs from blastocysts of HFD mice were significantly enriched for ferroptosis and autophagy, suggesting that ferroptosis and autophagy may be involved in the normal developmental process of preimplantation embryos.

MZT is the first critical developmental transition in mammalian early embryos, when the maternal mRNAs are degraded and zygotic genome begins transcription [43]. Abnormal MZT may lead to cell cycle arrest, developmental delay, and apoptosis [44, 45]. We performed enrichment analyses of inactivated DEGs in the HFD group, constructed PPI networks, and identified the most critical cluster. We demonstrated failed activation of 17 hub genes primarily involved in cell activation, cell adhesion, and response to extracellular stimulus in the HFD group. These results together indicated an abnormal MZT process after HFD-induced obesity.

Compared with other studies focusing on paternal obesity alone or combined parental obesity, our study focused on the effects of maternal obesity on the murine ovary and on early embryonic development. However, our study also had some limitations. Firstly, this study focused on an HFD-induced obesity, so our findings may not capture the effects of other obesity-inducing factors, such as high-sugar diets. In addition, sample sizes of preimplantation embryos at different stages for scRNA-seq remain small and dysregulated enrichment terms of DEGs should be further validated in vitro. Future work should expand the sample size and seek to comprehensively determine the epigenetic and gene expression changes in the oocytes and embryos of the offspring caused by maternal obesity. Finally, embryos for our scRNA-seq were obtained from in vivo fertilization, so the transcriptional landscape of HFD mice embryos may be affected by an abnormal oviductal and intrauterine environment.

Conclusions

In conclusion, our results revealed that HFD-induced maternal obesity impaired ovarian and oocyte function. Through our investigation, we provide novel insights into the changes in the transcriptional landscape of preimplantation embryos at different stages under the influence of HFD-induced obesity in maternal mice. These findings advance our understanding of the underlying mechanisms through which HFD-induced maternal obesity compromises ovarian and preimplantation embryo development. Importantly, our findings indicate that prepregnancy maternal weight interventions may benefit both mothers and preimplantation embryos.

Abbreviations

AUC	Area under the curve
DEG	Differentially expressed gene
GC	Granulosa cell
GO-BP	Gene Ontology biological process
GO-CC	Gene Ontology cellular component
GO-MF	Gene Ontology molecular function
GTT	Glucose tolerance test
hCG	Human chorionic gonadotropin
HFD	High-fat diet
KEGG	Kyoto Encyclopedia of Genes and Genomes
MZT	Maternal-to-zygotic transition
ND	Normal diet
PCA	Principal component analysis
PMSG	Pregnant mare serum gonadotropin
PPI	Protein-protein interaction
RT	Room temperature
scRNA-seq	Single-cell RNA sequencing
SD	Standard deviation
TC	Total cholesterol
TG	Triglycerides
ZGA	Zygote genome activation

Supplementary Information

The online version contains supplementary material available at https://doi.org/10.1186/s12958-024-01279-7.

Supplementary Material 1

Acknowledgements

We are particularly grateful to the staff who participated in this study and to the mice that were sacrificed for the experiment. Your tireless dedication made this study possible.

Author contributions

HG designed the study and revised the paper. QZ analyzed the data, performed the experiments, and wrote the manuscript. FL instructed experiments and helped to write the paper. HW directed the experiment. XW, YX, HD, HW, CX, LW, and JC participated in data analysis and performed the

experiments. TX, NL, XH, and MX helped to collect the samples. All authors read and approved the final manuscript.

Funding
This study was supported by the National Natural Science Foundation of China (81771586).

Data availability
No datasets were generated or analysed during the current study.

Declarations

Ethics approval and consent to participate
All animal procedures were approved by the Ethics Review Board for animal studies. All experiments were performed in accordance with the Declaration of Helsinki.

Competing interests
The authors declare no competing interests.

Received: 14 June 2024 / Accepted: 12 August 2024
Published online: 20 August 2024

References

1. Gambineri A, Laudisio D, Marocco C, Radellini S, Colao A, Savastano S. Female infertility: which role for obesity? Int J Obes Suppl. 2019;9:65–72.
2. Pasquali R, Pelusi C, Genghini S, Cacciari M, Gambineri A. Obesity and reproductive disorders in women. Hum Reprod Update. 2003;9:359–72.
3. Ng KYB, Cherian G, Kermack AJ, Bailey S, Macklon N, Sunkara SK, Cheong Y. Systematic review and meta-analysis of female lifestyle factors and risk of recurrent pregnancy loss. Sci Rep. 2021;11:7081.
4. Wang N, Luo LL, Xu JJ, Xu MY, Zhang XM, Zhou XL, Liu WJ, Fu YC. Obesity accelerates ovarian follicle development and follicle loss in rats. Metabolism. 2014;63:94–103.
5. van Swieten EC, van der Leeuw-Harmsen L, Badings EA, van der Linden PJ. Obesity and Clomiphene Challenge Test as predictors of outcome of in vitro fertilization and intracytoplasmic sperm injection. Gynecol Obstet Invest. 2005;59:220–4.
6. Sermondade N, Huberlant S, Bourhis-Lefebvre V, Arbo E, Gallot V, Colombani M, Fréour T. Female obesity is negatively associated with live birth rate following IVF: a systematic review and meta-analysis. Hum Reprod Update. 2019;25:439–51.
7. Jungheim ES, Schon SB, Schulte MB, DeUgarte DA, Fowler SA, Tuuli MG. IVF outcomes in obese donor oocyte recipients: a systematic review and meta-analysis. Hum Reprod. 2013;28:2720–7.
8. Li J, Wang S, Wang B, Wei H, Liu X, Hao J, Duan Y, Hua J, Zheng X, Feng X, Yan X. High-fat-diet impaired mitochondrial function of cumulus cells but improved the efficiency of parthenogenetic embryonic quality in mice. Anim Cells Syst (Seoul). 2018;22:243–52.
9. Lisle RS, Anthony K, Randall MA, Diaz FJ. Oocyte-cumulus cell interactions regulate free intracellular zinc in mouse oocytes. Reproduction. 2013;145:381–90.
10. Srinivasan M, Dodds C, Ghanim H, Gao T, Ross PJ, Browne RW, Dandona P, Patel MS. Maternal obesity and fetal programming: effects of a high-carbohydrate nutritional modification in the immediate postnatal life of female rats. Am J Physiol Endocrinol Metab. 2008;295:E895–903.
11. Maître JL. Mechanics of blastocyst morphogenesis. Biol Cell. 2017;109:323–38.
12. Xu R, Li C, Liu X, Gao S. Insights into epigenetic patterns in mammalian early embryos. Protein Cell. 2021;12:7–28.
13. Xue Z, Huang K, Cai C, Cai L, Jiang CY, Feng Y, Liu Z, Zeng Q, Cheng L, Sun YE, et al. Genetic programs in human and mouse early embryos revealed by single-cell RNA sequencing. Nature. 2013;500:593–7.
14. Velazquez C, Herrero Y, Bianchi MS, Cohen DJ, Cuasnicu P, Prost K, Marinoni R, Pascuali N, Parborell F, Abramovich D. Beneficial effects of metformin on mice female fertility after a high-fat diet intake. Mol Cell Endocrinol. 2023;575:111995.
15. Di Berardino C, Peserico A, Capacchietti G, Zappacosta A, Bernabò N, Russo V, Mauro A, El Khatib M, Gonnella F, Konstantinidou F et al. High-Fat Diet and Female Fertility across Lifespan: A Comparative Lesson from Mammal Models. Nutrients : 2022, 14.
16. Jukam D, Shariati SAM, Skotheim JM. Zygotic genome activation in vertebrates. Dev Cell. 2017;42:316–32.
17. Bettegowda A, Smith GW. Mechanisms of maternal mRNA regulation: implications for mammalian early embryonic development. Front Biosci. 2007;12:3713–26.
18. Kulie T, Slattengren A, Redmer J, Counts H, Eglash A, Schrager S. Obesity and women's health: an evidence-based review. J Am Board Fam Med. 2011;24:75–85.
19. Podrini C, Cambridge EL, Lelliott CJ, Carragher DM, Estabel J, Gerdin AK, Karp NA, Scudamore CL, Ramirez-Solis R, White JK. High-fat feeding rapidly induces obesity and lipid derangements in C57BL/6 N mice. Mamm Genome. 2013;24:240–51.
20. Tang LL, Tang XH, Li X, Yu HB, Xie ZG, Liu XY, Zhou ZG. Effect of high-fat or high-glucose diet on obesity and visceral adipose tissue in mice. Zhongguo Yi Xue Ke Xue Yuan Xue Bao. 2014;36:614–9.
21. Durmanova AK, Otarbayev NK, Kaiyrlykyzy A, Zhangazieva KK, Ibrayeva ZN, Donenbayeva GB, Zhusupova ZT, Saidakhmetov AS, Temirgaliyeva GS, Salykbayeva ZK, et al. [Ovarian reserve and adipokine levels in reproductive-aged obese women]. Ter Arkh. 2016;88:46–50.
22. Malhotra N, Bahadur A, Singh N, Kalaivani M, Mittal S. Does obesity compromise ovarian reserve markers? A clinician's perspective. Arch Gynecol Obstet. 2013;287:161–6.
23. Skaznik-Wikiel ME, Swindle DC, Allshouse AA, Polotsky AJ, McManaman JL. High-Fat Diet causes subfertility and compromised ovarian function Independent of obesity in mice. Biol Reprod. 2016;94:108.
24. Rao A, Satheesh A, Nayak G, Poojary PS, Kumari S, Kalthur SG, Mutalik S, Adiga SK, Kalthur G. High-fat diet leads to elevated lipid accumulation and endoplasmic reticulum stress in oocytes, causing poor embryo development. Reprod Fertil Dev. 2020;32:1169–79.
25. Luzzo KM, Wang Q, Purcell SH, Chi M, Jimenez PT, Grindler N, Schedl T, Moley KH. High fat diet induced developmental defects in the mouse: oocyte meiotic aneuploidy and fetal growth retardation/brain defects. PLoS ONE. 2012;7:e49217.
26. Maffeis C, Morandi A. Effect of maternal obesity on Foetal Growth and Metabolic Health of the offspring. Obes Facts. 2017;10:112–7.
27. Matorras R, Exposito A, Ferrando M, Mendoza R, Larreategui Z, Laínz L, Aranburu L, Andrade F, Aldámiz-Echevarria L, Ruiz-Larrea MB, Ruiz-Sanz JI. Oocytes of women who are obese or overweight have lower levels of n-3 polyunsaturated fatty acids compared with oocytes of women with normal weight. Fertil Steril. 2020;113:53–61.
28. Leary C, Leese HJ, Sturmey RG. Human embryos from overweight and obese women display phenotypic and metabolic abnormalities. Hum Reprod. 2015;30:122–32.
29. Leong I. Obesity: link between maternal obesity and offspring is STELLA. Nat Rev Endocrinol. 2018;14:189.
30. Gu TP, Guo F, Yang H, Wu HP, Xu GF, Liu W, Xie ZG, Shi L, He X, Jin SG, et al. The role of Tet3 DNA dioxygenase in epigenetic reprogramming by oocytes. Nature. 2011;477:606–10.
31. Liu D, Wang X, He D, Sun C, He X, Yan L, Li Y, Han JJ, Zheng P. Single-cell RNA-sequencing reveals the existence of naive and primed pluripotency in pre-implantation rhesus monkey embryos. Genome Res. 2018;28:1481–93.
32. Shi J, Chen Q, Li X, Zheng X, Zhang Y, Qiao J, Tang F, Tao Y, Zhou Q, Duan E. Dynamic transcriptional symmetry-breaking in pre-implantation mammalian embryo development revealed by single-cell RNA-seq. Development. 2015;142:3468–77.
33. Sun S, Cao C, Li J, Meng Q, Cheng B, Shi B, Shan A. Lycopene modulates placental health and fetal development under High-Fat Diet during pregnancy of rats. Mol Nutr Food Res. 2021;65:e2001148.
34. Wang B, Shi M, Yu C, Pan H, Shen H, Du Y, Zhang Y, Liu B, Xi D, Sheng J, et al. NLRP3 inflammasome-dependent pathway is involved in the pathogenesis of polycystic ovary syndrome. Reprod Sci. 2024;31:1017–27.
35. Bernhardt L, Dittrich M, El-Merahbi R, Saliba AE, Müller T, Sumara G, Vogel J, Nichols-Burns S, Mitchell M, Haaf T. El Hajj N: A genome-wide transcriptomic analysis of embryos fathered by obese males in a murine model of diet-induced obesity. Sci Rep 2021, 11:1979.
36. Hedegger K, Philippou-Massier J, Krebs S, Blum H, Kunzelmann S, Förstemann K, Gimpfl M, Roscher AA, Ensenauer R, Wolf E, Dahlhoff M. Sex-specific programming effects of parental obesity in pre-implantation embryonic development. Int J Obes (Lond). 2020;44:1185–90.

37. Campbell JM, Lane M, Owens JA, Bakos HW. Paternal obesity negatively affects male fertility and assisted reproduction outcomes: a systematic review and meta-analysis. Reprod Biomed Online. 2015;31:593–604.
38. Lane M, Zander-Fox DL, Robker RL, McPherson NO. Peri-conception parental obesity, reproductive health, and transgenerational impacts. Trends Endocrinol Metab. 2015;26:84–90.
39. Finger BJ, Harvey AJ, Green MP, Gardner DK. Combined parental obesity negatively impacts preimplantation mouse embryo development, kinetics, morphology and metabolism. Hum Reprod. 2015;30:2084–96.
40. Bakos HW, Henshaw RC, Mitchell M, Lane M. Paternal body mass index is associated with decreased blastocyst development and reduced live birth rates following assisted reproductive technology. Fertil Steril. 2011;95:1700–4.
41. Binder NK, Mitchell M, Gardner DK. Parental diet-induced obesity leads to retarded early mouse embryo development and altered carbohydrate utilisation by the blastocyst. Reprod Fertil Dev. 2012;24:804–12.
42. Bermejo-Alvarez P, Rosenfeld CS, Roberts RM. Effect of maternal obesity on estrous cyclicity, embryo development and blastocyst gene expression in a mouse model. Hum Reprod. 2012;27:3513–22.
43. Li L, Lu X, Dean J. The maternal to zygotic transition in mammals. Mol Aspects Med. 2013;34:919–38.
44. Yang Y, Zhou C, Wang Y, Liu W, Liu C, Wang L, Liu Y, Shang Y, Li M, Zhou S, et al. The E3 ubiquitin ligase RNF114 and table 1 degradation are required for maternal-to-zygotic transition. EMBO Rep. 2017;18:205–16.
45. Zhao BS, Wang X, Beadell AV, Lu Z, Shi H, Kuuspalu A, Ho RK, He C. M(6) A-dependent maternal mRNA clearance facilitates zebrafish maternal-to-zygotic transition. Nature. 2017;542:475–8.

Publisher's Note